Hard-sphere statistics along the metastable amorphous branch

M. D. Rintoul and S. Torquato
Princeton Materials Institute and Department of Civil Engineering and Operations Research, Princeton University, Princeton, New Jersey 08540
(Received 10 March 1998)

Using simulation techniques that we discussed in a previous work, we create random dense hard-sphere systems above the freezing point (i.e., along the metastable branch) and measure key quantities that characterize the structure for such high densities. These include certain statistics of the void space, nearest-neighbor statistics, and the mean coordination number. Our numerical results turn out to be generally in very good agreement with recent theoretical predictions. [S1063-651X(98)07707-1]

PACS number(s): 61.20.−p

I. INTRODUCTION

Dense systems of randomly packed hard spheres have been the subject of much study recently. This is due in part to its usefulness as a model of such physical systems as simple liquids [1], glasses [2], colloidal dispersions, and particulate composites [3]. Since the short-range repulsion between particles in dense systems generally determines the structure, the hard-sphere model turns out to approximate well the structure of such systems even when interparticle attraction is present. The hard-sphere system is also appealing since, despite its simplicity and much theoretical and computational work, many open questions remain regarding the structure over the full density range.

One of the primary difficulties in studying dense random hard-sphere systems is that of determining whether the systems are truly random. Bernal [4] was one of the first to study such a system via physical experiment, in which plasticene spheres were compressed together in order to get an effective ''Voronoi tessellation'' of the random-sphere system. He also used an actual ''ball and stick'' approach model to study the system. The practical difficulties inherent in these methods make them of limited general use. Finney [5] carried out some of the first Monte Carlo calculations to study dense hard-sphere systems. Almost all early techniques were based around the Voronoi approach, but they also focused on the radial distribution function as a means of determining randomness. This was based on the difference between the radial distribution function of the crystalline and random systems.

There has also been much work done on so-called ''deposition models,'' in which spheres are deposited sequentially onto a random surface according to some given rule [6]. In general, such methods produce dense random systems, but do not have the same characteristics that are associated with systems in which the particles are not ''locked into place.'' Moreover, deposition models do not produce packings that are as dense as algorithms that allow particle movement [7,8].

As the hard-sphere system was studied, the thermodynamics of the system was emphasized and its complete phase diagram was investigated with the help of numerical simulations. In Fig. 1, one can see that there are four main branches in the phase diagram. The first branch goes from $\phi=0$ to the freezing point $\phi_f \approx 0.494$ and represents the stable fluid (disordered) phase. A tie line representing a mixed ordered and disordered phase joins the freezing point and the melting point $\phi_m \approx 0.545$. Above the melting point, the system is in a crystalline phase that ends at a close-packed face-centered cubic at $\phi \approx 0.74$. However, the random dense hard-sphere phase is not represented by any of these lines, but instead is a metastable extension of the fluid branch that extends past the freezing point, and is conjectured to end at the random close-packing (RCP) state $\phi_c \approx 0.644$. Roughly speaking, the RCP state is the densest possible random packing (see Ref. [9] for a more precise definition). There is a complete range of partially disordered states that a hard-sphere system can be in, both equilibrium and nonequilibrium, but current studies of dense random hard-sphere systems are primarily concerned with the metastable extension of the fluid branch.

In the context of the hard-sphere phase diagram, one can see that the fundamental problem in creating metastable dense systems is to ensure that the system is truly random. Unfortunately, there is no perfect measure of order or disorder in a system, and systems were generally thought to be disordered as long as the the radial distribution function did not begin to show clear signs associated with a fcc crystal. However, we showed in previous work [10] that small

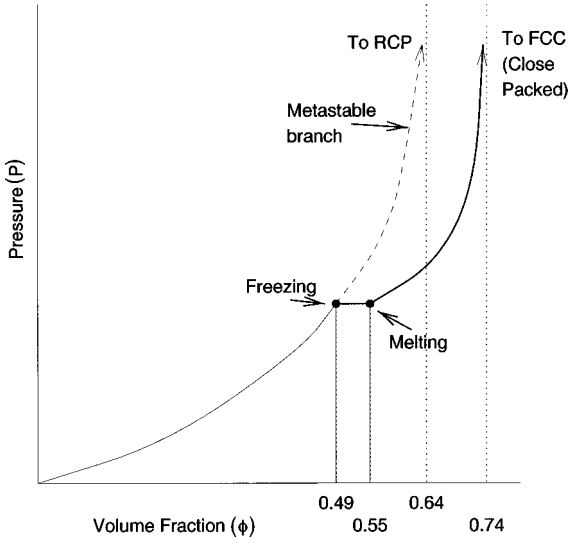

FIG. 1. Phase diagram for the hard-sphere system.

amounts of crystallization, which were imperceptible to the radial distribution function, can indeed affect the physical properties, such as pressure, in the system.

In order to quantify the degree of local order (disorder) in the system, we borrowed the concept of an order parameter Q_6 from Steinhart, Nelson, and Ronchetti [11]. The order parameter Q_6 corresponds to a rotationally invariant average over all bonds, which is nonzero in the presence of any type of crystallization, and zero for a completely disordered system. By monitoring the behavior of Q_6 to ensure that no crystallites were forming, we were able to both equilibrate our hard-sphere systems and be assured that they remained random. We suspect that many previous studies that attempted to produce random packings of spheres solely based on the radial distribution function may well contain crystallites.

Using the aforementioned concept of an order parameter to characterize hard-sphere systems, we found a precise *quantitative* means of creating dense random hard-sphere systems that correspond to the metastable amorphous branch of the phase diagram [10], which heretofore had been lacking. We were then able to establish a number of new results related to dense metastable hard-sphere systems. These results include precise values of the pressure along the branch, a precise value of random close packing ϕ_c (≈ 0.644), and a lack of the existence of a thermodynamic glass transition.

In this paper, we use the same techniques to create dense random hard-sphere systems and measure key statistical properties of these systems. First, we calculate the void nearest-neighbor distribution functions $E_V(r)$ and $H_V(r)$. These two functions describe the geometry of the cavities in the hard-sphere system and were originally used in scaled-particle theory to determine the system thermodynamics [12]. Using $H_V(r)$, we will also calculate the mean pore size $\langle \delta \rangle$ and associated fluctuations. Such pore length scales determine transport properties of the systems, such as the mean survival time of Brownian particles diffusing in a system of traps [13]. We emphasize that this, to our knowledge, is the first computer simulation of these quantities above the freezing point, along the metastable branch. Finally, we will calculate the first and second moments of the particle nearest-neighbor functions as well as an effective mean coordination number associated with these dense packings. The latter quantities are key in characterizing the system as it approaches the RCP state. We will also use our simulation results to compare to previous theoretical predictions [9,14].

In Sec. II we precisely define the void nearest-neighbor quantities $E_V(r)$ and $H_V(r)$, and calculate them as well as lower-order moments using computer-simulation techniques. They are then compared to theoretical expressions. We discuss and compute the particle nearest-neighbor statistics in Sec. III, such as the mean nearest-neighbor distance and associated variance, and the mean coordination number. Finally, in Sec. IV we make concluding remarks.

II. VOID STATISTICS

In what follows, we consider a statistically isotropic distribution of identical hard spheres of diameter σ. Let ϕ represent the volume fraction of the spheres. The void nearest-neighbor quantities $H_V(r)$ and $E_V(r)$ have been extensively studied [12,14] and are defined as follows:

$$H_V(r)dr = \text{probability that at an arbitrary point in the system, the center of the nearest particle, lies at a distance between } r \text{ and } r+dr. \tag{1}$$

$$E_V(r) = \text{probability of finding a region that is a circular cavity of radius } r \text{ (centered at some arbitrary point), empty of disk centers.} \tag{2}$$

The quantity $H_V(r)$ can be interpreted as being the interfacial area per unit volume of a system of possibly overlapping spheres of radius r centered at each of the actual sphere centers. Similarly, $E_V(r)$ has the interpretation of the volume fraction of space occupied by a system of possibly overlapping spheres of radius r centered at each of the actual sphere centers. The pore-size distribution $P(\delta)$ has been defined in terms of H_V [13] according to the relation

$$P(\delta) = \frac{H_V(\delta - \sigma/2)}{1-\phi}. \tag{3}$$

Then, the mean pore-size distribution $\langle \delta \rangle$, and higher-order moments can be defined by

$$\langle \delta^n \rangle = \int \delta^n P(\delta) d\delta. \tag{4}$$

The two quantities $H_V(r)$ and $E_V(r)$ are not independent, but are related by the expression

$$E_V(r) = 1 - \int_0^r H_V(x)dx. \tag{5}$$

It is easy to see, from the physical definitions given above, that

$$E_V(r) = 1 - \rho \frac{4\pi r}{3}, \quad 0 \leq r \leq \sigma/2, \tag{6}$$

and

$$H_V(r) = \rho 4\pi r^2, \quad 0 \leq r \leq \sigma/2, \tag{7}$$

where ρ is the number density of particles.

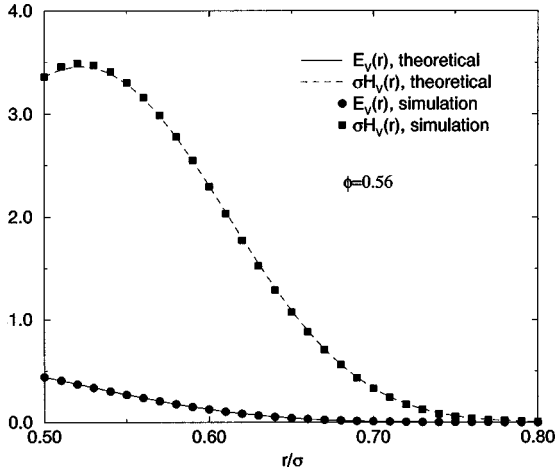

FIG. 2. Comparison of the simulations of $E_V(r)$ and $H_V(r)$ to the theoretical expressions (12) and (13) for $\phi=0.56$.

Torquato [9] has obtained an accurate analytical approximation for the intimately related conditional nearest-neighbor function $G_V(r)$ [14] for volume fractions up to the freezing point:

$$G_V(x)=a_0+\frac{a_1}{x}+\frac{a_2}{x^2}, \tag{8}$$

where

$$a_0=\frac{1+\phi+\phi^2-\phi^3}{(1-\phi)^3}, \tag{9}$$

$$a_1=\frac{\phi(3\phi^2-4\phi-3)}{2(1-\phi)^3}, \tag{10}$$

$$a_2=\frac{\phi^2(2-\phi)}{2(1-\phi)^3}. \tag{11}$$

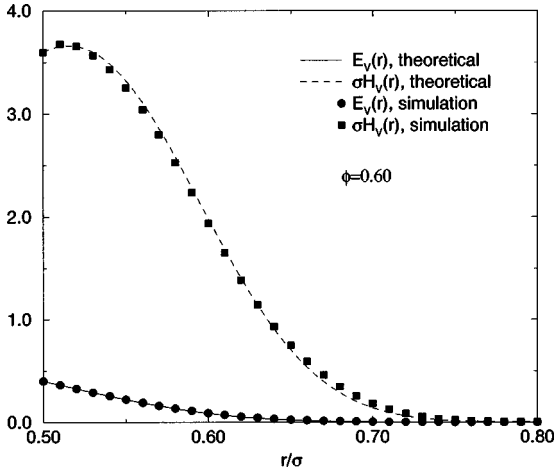

FIG. 3. Comparison of the simulations of $E_V(r)$ and $H_V(r)$ vs scaled distance r/σ to the theoretical expressions (12) and (13) for $\phi=0.60$.

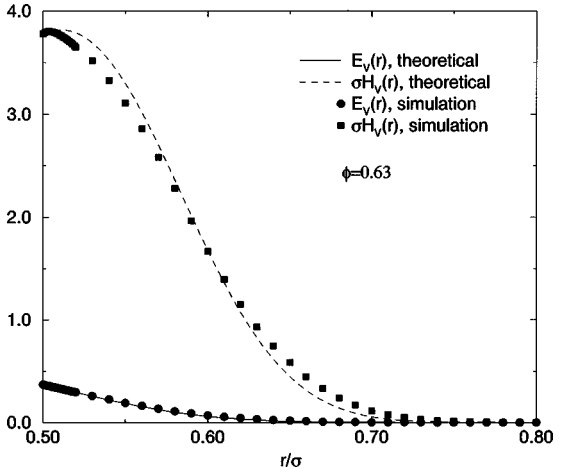

FIG. 4. Comparison of the simulations of $E_V(r)$ and $H_V(r)$ vs scaled distance r/σ to the theoretical expressions (12) and (13) for $\phi=0.63$.

and $x=r/\sigma$. The corresponding expressions for $E_V(x)$ and $H_V(x)$, using the exact interrelations [14], are given by

$$E_V(x)=(1-\phi)\exp[-\phi(8a_0x^3+12a_1x^2+24a_2x+a_3)], \tag{12}$$

$$H_V(x)=24\phi(1-\phi)(a_0x^2+a_1x+a_2)\exp[-\phi(8a_0x^3+12a_1x^2+24a_2x+a_3)], \tag{13}$$

where

$$a_3=-(a_0+3a_1+12a_2). \tag{14}$$

As observed by Torquato [9], the void nearest-neighbor functions are fundamentally different than the ''particle'' nearest-neighbor functions (described in the next section) since the former, unlike the latter, do not vanish or diverge at the RCP state. This implies that the functional nature of the particle quantities below and above the freezing density must be different [9]. Since the void quantities are nonsingular at

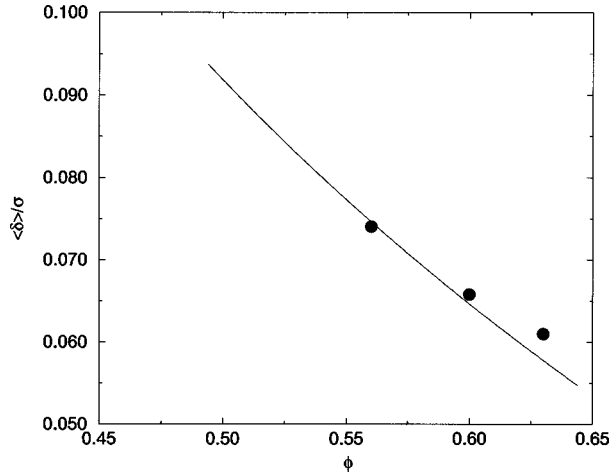

FIG. 5. Comparison of the simulations of the dimensionless mean pore size $\langle\delta\rangle/\sigma$ vs scaled distance r/σ to the theoretical expression (4), with $n=1$ and H_V given by Eq. (13), for several values of ϕ.

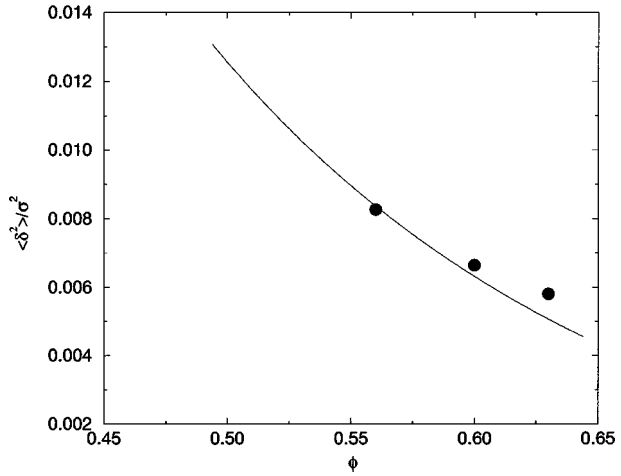

FIG. 6. Comparison of the simulations of the dimensionless second moment of the pore-size distribution $\langle \delta^2 \rangle / \sigma^2$ to the theoretical expression (4), with $n=2$ and H_V given by Eq. (13), for several values of ϕ.

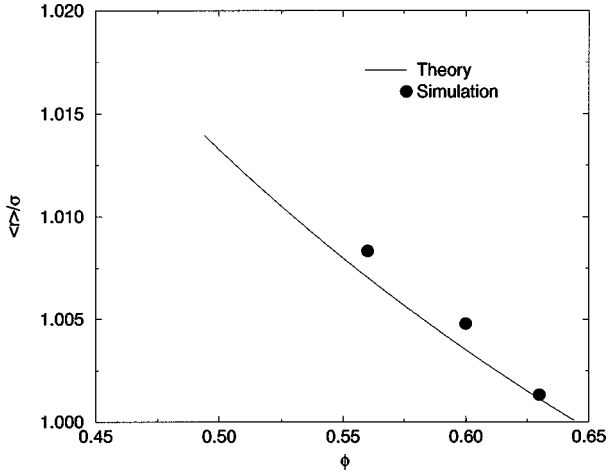

FIG. 7. Comparison of the simulations of the dimensionless mean nearest-neighbor distance $\langle r \rangle / \sigma$ to the theoretical expression (16), with $n=1$ and H_P given by Eq. (17), for several values of ϕ.

RCP, it seems reasonable that by analytically continuing the expressions (8), (12), and (13) above the freezing point, they may provide useful estimates of the void quantities along the metastable branch. This ansatz will be tested against our simulation results.

Simulations to determine $E_V(r)$ and $H_V(r)$ were performed at various volume fractions between the freezing point ($\phi_f = 0.494$) and random close packing ($\phi_c = 0.644$) by creating the systems using the techniques described in our earlier papers [10]. The volume and area for various values of r was then determined using the algorithm specified by Dodd and Theodorou [15], with minor performance modifications. Each simulation was performed on 2000-particle systems using periodic boundary conditions.

The resulting plots of $E_V(r)$ and $H_V(r)$ compared to theory are shown in Figs. 2–4. The first plot, which depicts the results for $\phi = 0.56$, shows extremely close agreement with theory. However, the data in Fig. 3 also shows very good agreement with theory at the higher value of $\phi = 0.60$. Figure 4 shows that even at $\phi = 0.63$, a value very close to random close packing, the theoretical expressions do not break down significantly, in contrast to previous predictions.

The data for $H_V(r)$ were used to calculate the pore-size distribution $P(\delta)$, and the mean pore size $\langle \delta \rangle$ and mean pore-size fluctuations $\langle \delta^2 \rangle$ were calculated from $P(\delta)$. The moments $\langle \delta \rangle$ and $\langle \delta^2 \rangle$ are plotted in Figs. 5 and 6, respectively, and are compared to the theoretical predictions as computed from Eqs. (3), (4), and (13). Noting the scales of the figures, the theoretical predictions are seen to be in excellent agreement with the simulation data.

III. PARTICLE NEAREST-NEIGHBOR STATISTICS

The particle nearest-neighbor quantities $H_P(r)$ and $E_P(r)$ are similar to the void nearest-neighbor quantities, but instead of the reference point as an arbitrary point in the system, it is a particle center [14]. Specifically, $H_P(r)$ is defined as

$$H_P(r)dr = \text{probability that at an arbitrary particle center in the system, the center of the nearest particle, lies at a distance between } r \text{ and } r+dr. \quad (15)$$

This is just the distribution of nearest-neighbor distances. From this quantity, one can define the mean nearest-neighbor distance $\langle r \rangle$ and its higher moments as

$$\langle r^n \rangle = \int_0^\infty r^n H_P(r) dr. \quad (16)$$

A theoretical approximation for $H_P(r)$ from the freezing point ϕ_f to RCP ϕ_c was explicitly given by Torquato in Eq. (43) of Ref. [9], which states that

$$H_P(r) = 24\phi(a_0 x^2 + a_1 x + a_2)\exp\{-\phi[8a_0(x^3-1) + 12a_1(x^2-1) + 24a_2(x-1)]\} \quad (x \geq 1), \quad (17)$$

where

$$a_0 = 1 + 4\phi g_f(1)\frac{(\phi_c - \phi_f)}{(\phi_c - \phi)}, \quad (18)$$

$$a_1 = \frac{3\phi - 4}{2(1-\phi)} + 2(1-3\phi)g_f(1)\frac{(\phi_c - \phi_f)}{(\phi_c - \phi)}, \quad (19)$$

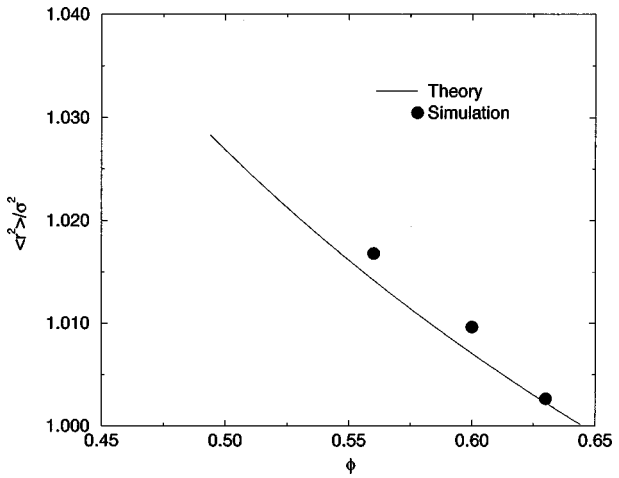

FIG. 8. Comparison of the simulations of the dimensionless second moment $\langle r^2\rangle/\sigma^2$ to the theoretical expression (16), with $n=2$ and H_P given by Eq. (17), for several values of ϕ.

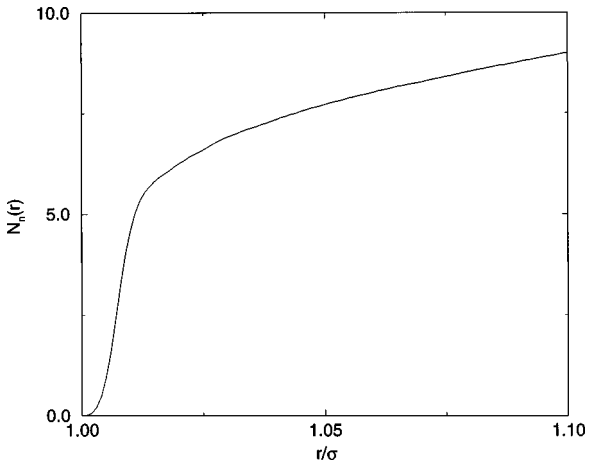

FIG. 9. Coordination number (average number of neighboring sphere centers) as a function of distance for $\phi=0.63$. Note the sharp change in the behavior of the function at a point corresponding to about six neighbors.

$$a_2=\frac{2-\phi}{2(1-\phi)}+(2\phi-1)g_f(1)\frac{(\phi_c-\phi_f)}{(\phi_c-\phi)}, \qquad (20)$$

and $g_f(1)=(1-\phi_f/2)/(1-\phi_f)^3$ denotes the contact value of the radial distribution function at the freezing packing fraction $\phi_f=0.494$.

In general, it is much more difficult to get the entire distribution of particle nearest-neighbor quantities than the void nearest-neighbor quantities. This is due to the fact that the sampling for the particle quantities is limited to the number of particles in your system, while there are effectively an infinite number of void points to sample from. Because of this, we will concentrate on the first and second moments of $H_P(r)$, and not the entire function.

In Fig. 7 we compare the mean nearest-neighbor distance $\langle r\rangle$, obtained from our simulations to the one computed from Eqs. (16) and (17) for various values of the volume fraction ϕ. Here we see that the values lie very close to the approximation given by Eq. (16) with $n=1$. Similarly, Fig. 8 gives corresponding results for the second moment $\langle r^2\rangle$. The agreement with theory [Eq. (16) with $n=2$ and Eq. (17)] is also quite good.

For a hard-sphere system in equilibrium, the coordination number (average number of interparticle contacts) is *strictly zero except at the RCP state*. Therefore, we instead compute the mean number of neighbors $N_n(r)$, where $N_n(r)$ is defined as the mean number of sphere centers *located within a distance r from a random sphere center*. Even though $N_n(\sigma)=0$ for all values used in this simulation, we can plot $N_n(r)$ for values close to σ to get an idea of what a reasonable value for the coordination number should be. Figure 9 shows the results for $\phi=0.63$, very close to RCP. We see a very sharp rise up to a value of approximately six, and then a slow rise to slightly higher values. This implies that each particle has six neighbors a very short distance away (note the scale in Fig. 9) corresponding to an approximate coordination number of six. As $\phi\to\phi_c$, it is expected that $N_n(r)$ will plateau even faster after the initial steep rise. It is well known experimentally that the coordination number of random-sphere packings is approximately six [16].

IV. CONCLUSIONS

Theoretical predictions for nearest-neighbor void and particle statistics along the metastable amorphous branch are shown to be very accurate when compared to computer simulations, even at values close to RCP. This is in contrast with many previous theoretical predictions of hard-sphere systems that tend to break down at higher densities. We note that the void statistics, while somewhat more geometrically complicated than the particle statistics, are easier to measure than the particle quantities. Finally, we have shown that as dense random hard-sphere systems approach the RCP state, the coordination number tends toward a limiting value of approximately six, consistent with experimental measurements on random-sphere packings.

[1] J. P. Hansen and I. R. McDonald, *Theory of Simple Liquids* (Academic, London, 1986).
[2] R. Zallen, *The Physics of Amorphous Solids* (Wiley, New York, 1983).
[3] S. Torquato and F. Lado, Phys. Rev. B **33**, 6428 (1986).
[4] J.D. Bernal, Nature (London) **183**, 141 (1959); Proc. R. Soc. London, Ser. A **280**, 299 (1964).
[5] J. L. Finney, Proc. R. Soc. London, Ser. A **319**, 479 (1970).
[6] R. Jullien and P. Meakin, Europhys. Lett. **4**, 1385 (1987).
[7] W. S. Jodrey and E. M. Tory, Phys. Rev. A **32**, 2347 (1985).
[8] A. S. Clarke and J. D. Wiley, Phys. Rev. B **35**, 7350 (1987).
[9] S. Torquato, Phys. Rev. E **51**, 3170 (1995).
[10] M. D. Rintoul and S. Torquato, Phys. Rev. Lett. **77**, 4198 (1996); J. Chem. Phys. **105**, 9258 (1996); **107**, 2698 (1997).

[11] P. J. Steinhardt, D. R. Nelson, and M. Ronchetti, Phys. Rev. B **28**, 784 (1983).
[12] H. Reiss, H. L. Frisch, and J. L. Lebowitz, J. Chem. Phys. **31**, 369 (1959).
[13] S. Torquato and M. Avellaneda, J. Chem. Phys. **95**, 6477 (1991).
[14] S. Torquato, B. Lu, and J. Rubinstein, Phys. Rev. A **41**, 2059 (1990).
[15] L. Dodd and D. Theodorou, Mol. Phys. **72**, 1313 (1991).
[16] J. D. Bernal and J. Mason, Nature (London) **188**, 908 (1964).